Aliphatic amines modified CoO nanoparticles for catalytic oxidation of aromatic hydrocarbon with molecular oxygen

LIU Meng [a,b], SHI Song [a, #], ZHAO Li [a,b], CHEN Chen [a,c], GAO Jin [a], XU Jie [a,*]

[a] State Key Laboratory of Catalysis, Dalian Institute of Chemical Physics, Chinese Academy of Sciences, Dalian National Laboratory for Clean Energy, Dalian 116023, Liaoning, China

[b] University of Chinese Academy of Sciences, Beijing 100049, China

[c] School of Materials Science & Chemical Engineering, Ningbo University, Ningbo 315211, Zhejiang, China.

Abstract: The surface modification of metal oxide with organic modifier showed potential application in enhanced catalysis performance, and a hydrophobic CoO nanoparticle with amine modification on the surface owning water contact angle of 143° was synthesized. The catalyst was characterized by XRD, TGA, FT-IR, HR-TEM, XPS, etc. And it showed better performance than the hydrophilic commercial CoO nanoparticle in the process of aromatic hydrocarbon oxidation. After handled with the amines modification method, the commercial CoO also changed to hydrophobic and showed an improved conversion of ethylbenzene. The surface modification of CoO with amines brought the hydrophobicity property, which could provide a reference for other hydrophobic catalysts design.

The selective oxidation of hydrocarbons to oxygen-containing compounds with dioxygen is an important process in both academic research and the industry production [1-3]. The difficulties of this process lie in the activation of the inert C-H bond and the selectivity to the alcohols and ketones, which are more active than the hydrocarbons [4,5]. The metal oxides nanoparticles are one of the efficient catalysts for the hydrocarbon oxidation. Several metal oxides have been developed to improve the efficiency of this process, including Mn_3O_4 [6], CoO_x [7] and CuO_x [8,9], etc. Among these catalyst systems, the CoO_x showed good performance, especially the nano-sized particles. In regard to the CoO_x, the porosity [10], particle size [11] and co-component [12] of the nanoparticles has been researched. There are many other aspects that could help to enhance the reaction rate of a heterogeneous catalysis, the electronic state [13] and the microenvironment [14], etc. Due to the nature of the hydrocarbon oxidation process, the surface hydrophobicity of the catalyst gained the advantage in the oxidation process [15-19]. The cobalt oxides nanoparticles exhibited hydrophilic properties for the polar hydroxyl groups on the surface. In our previous

report [15,17] silica was act as the co-component and a common strategy with organosilane modification was applied to make the surface hydrophobic. However, the direct hydrophobic modification of the cobalt oxide nanoparticles, which acted as active site, was rarely studied. It is a challenging task to direct modification of the nanoparticles into hydrophobic surface.

Organic modification strategy is an important method to modify the catalyst's surface [20,21]. Several research teams have reported the modification method to improve or tune the selectivity of a certain reaction. In particular, when modified with organic modifier, the metal oxides, such as CeO_2, TiO_2 and MnO_2 were promoted to get enhanced reaction performance, and the modifiers include organophosphonic acid [22], carboxylates [23] and 2-cyanopyridine [24], et al. Our team has previously reported the green modification of the MnO_2 surface with carboxylates to adjust the selectivity of desired product [23]. However, little attention is paid to the modification of CoO_x with aliphatic amines for aromatic hydrocarbon oxidation.

Herein, the amines modified CoO nanoparticle was synthesized through the solvothermal approach to decompose a cobalt-oleate complex in the solvent of 2-octanol and amines system. The amines which acted as organic modifier was in-situ introduced in the CoO during the synthesis process, the CoO nanoparticle exhibited the hydrophobic characteristic and showed good performance in the aromatic hydrocarbon oxidation process. Two similar CoO nanoparticles were obtained with butylamine (BA) and dodecylamine (DA) coating on the surface, which denoted as BA-CoO and DA-CoO, respectively.

XRD patterns in Fig. 1 showed the bulk phase of the as-synthesized nanoparticles. Both BA-CoO and DA-CoO showed the main peaks at the (111), (200) and (220) planes of cubic CoO with a rock salt structure as the commercial CoO, confirming the nanoparticles were in CoO phase. This was also confirmed by the HR-TEM (Fig. 2d) which showed a d-spacing value of 0.25 nm corresponding to CoO (111). The peak intensity of DA-CoO is weaker than BA-CoO and commercial CoO, which was attributed to the smaller particle size of DA-CoO in keeping with the TEM results showed in Fig. 2.
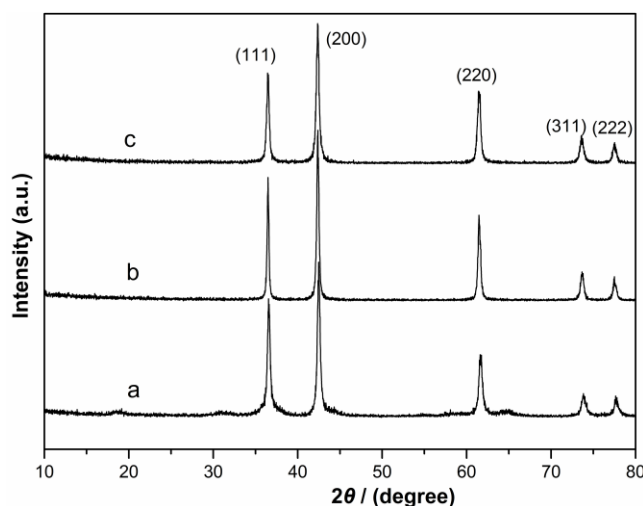

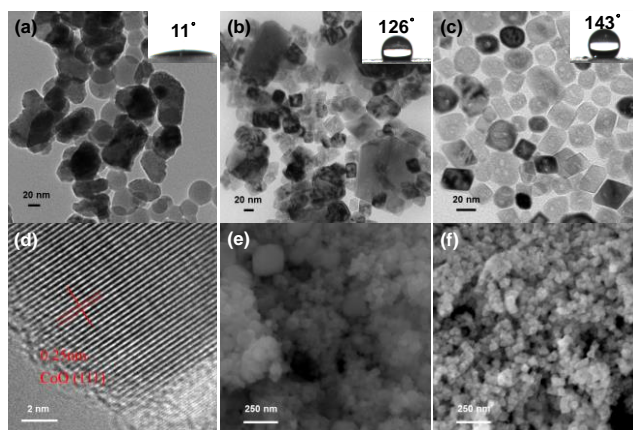**Fig. 1.** XRD patterns of (a) commercial CoO; (b) BA-CoO; (c) DA-CoO

Fig. 2. TEM images of the (a) commercial CoO, (b) BA-CoO, (c) DA-CoO; (d) HRTEM of the BA-CoO; SEM images of the (e) BA-CoO, (f) DA-CoO; (The insets are the images of sessile water droplets on the material film)

The morphology of the particle and distribution of the particle size could be directly observed through TEM characterization. As seen TEM image from Fig. 2c and SEM image from Fig. 2f, the DA-CoO nanoparticle has morphology of a nano-cubic and an average size of about 25 nm (Fig. S1). Similarity, the BA-CoO is also a nano-cubic but the size distribution is broad (Fig. S2). This difference may be caused by the stronger basicity of butylamine which accelerated the decomposition of Co-oleate and resulted in the larger size and broad distribution of BA-CoO. The commercial CoO has an average size of 49 nm similar as the BA-CoO (Fig. S3). This excluded the size effect on the reaction (vide infra). The hydrophobicity of the catalyst was characterized by the water droplet contact angle measurements (WCA). The insets in Fig. 2 are the images of sessile water droplets on the material film. The commercial CoO is hydrophilic which has a WCA value below 20°. In contrast, the BA-CoO has a WCA value of 126° and the DA-CoO reached 143°. This may be accounted for the catalytic difference (vide infra). The difference in WCA also suggested the surface of the as-synthesized CoO was coated by amines.
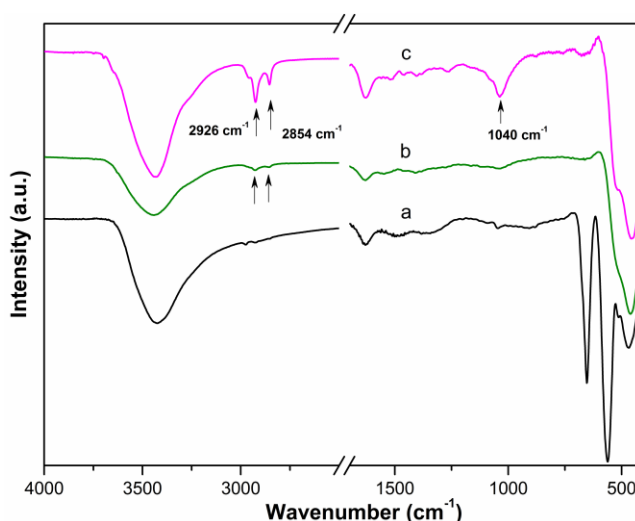

Fig. 3. FT-IR spectra of (a) commercial CoO; (b) BA-CoO; (c) DA-CoO

The existence of amines on the surface of the as-synthesized CoO was identified by Fourier transform infrared spectroscopy (FT-IR) and X-ray photoelectron spectroscopy (XPS). The nanoparticles were washed with hexane and ethanol until the FT-IR spectra unchanged to remove the organic compounds adsorbed (Fig. S4, S5). The three samples presented broad absorption peaks at 3440 cm^{-1} and 1630 cm^{-1}, which accounted for the O-H stretching vibration and bending mode of the adsorbed water [25]. The peaks of 2854 cm^{-1} and 2926 cm^{-1} in the FT-IR spectrum of DA-CoO are attributed to C–H band vibration absorption. The peak at about 1040 cm^{-1} could be ascribed to the stretching vibrations of C–N bonds [26,27], and the peaks between 1300 and 1600 cm^{-1} could be due to the –NH_2 [28], which proved the existence of the amines on the surface (Fig. 3c). As a contrast, no peaks attributed to C–H band vibration absorption in commercial CoO were observed. In comparison with DA-CoO, weaker absorption peak appeared in BA-CoO, which attributed to the shorter length of butylamine than dodecylamine. Compared the BA-CoO with the DA-CoO, the increase of WCA could also be attributed to the longer length of dodecylamine than butylamine (vide supra).

The results of XPS measurements confirmed that the amines existed on the nanoparticle's surface for the presence of N1s peak (Fig. S7, S8). The compositions of the samples are presented in Table S1. The N content in each sample is less than 1%, which is in consistence with the TGA curve (Fig. S9). The TGA results showed a weight loss of 7% of the DA-CoO and nearly no weight loss of the commercial CoO. For DA-CoO, there was an obvious weight loss at 410°C which is much higher than the boiling temperature of 2-octanol and dodecylamine, for which are 178°C and 259°C respectively. Furthermore, both the TGA results of 2-octanol and dodecylamine showed a rapid weight loss blew 200°C (Fig. S10). It proved the interaction between the amines and CoO nanoparticles to some extent. Though the XRD results confirmed the nanoparticles are in CoO phase, in the XPS measurement, the Co(III) was detected. The Co 2p XPS spectra, as illustrated in Fig. 4, were comprised of two main peaks at about 780.0 eV and 796.5 eV, assigned
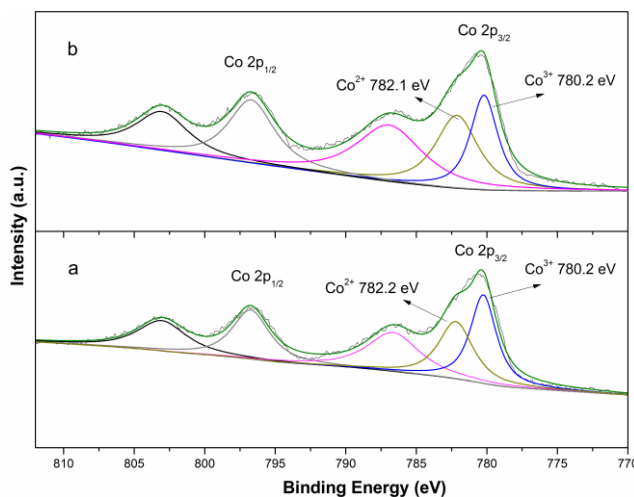

Fig. 4. Co 2p XPS spectra of (a) DA-CoO; (b) BA-CoO

to Co $2p_{3/2}$ and Co $2p_{1/2}$, respectively. Fitting the curves according to the characteristics of the cobalt oxides [29-31], the Co(III)/Co(II) ratio of the two samples are depicted in Table S1. Co(III) existed on the surface of the samples, which implied partial of the CoO nanoparticle's surface turn to high valence Co(III), the results of FT-IR are in keeping with the XPS. The peak located at 460 cm^{-1} is attributed to the stretching vibration of Co-O bond in CoO with a rock-salt structure, while the two bands observed at 646 and 522 cm^{-1} are characteristic vibrations of Co(II)-O and Co(III)-O bond in Co_3O_4 [25, 32]. It implied the existence of small amount Co(III) in the as-synthesized CoO. The existence of Co(III) might do favor to the hydrocarbon oxidation [31], which can also be a factor for the enhancement of the catalytic performance.

Selective oxidation of ethylbenzene was carried out as the model reaction with the above materials as catalysts (Table 1). A remarkable difference was observed between the hydrophilic and hydrophobic catalysts. With commercial hydrophilic CoO particles, the conversion was only 18% (entry 3), while in contrast, the hydrophobic DA-CoO showed a high conversion of 53% (entry 2), which is almost twofold higher compared with the commercial CoO particles. In addition, the selectivity of acetophenone also increased from 69 to 78%. In the selective oxidation of hydrocarbons, alcohol is one of the primary oxidation products, which can be further oxidized to ketone. Higher selectivity for ketones means that hydrophobic DA-CoO has stronger oxidation ability. To investigate the vital factors of catalytic differences between commercial CoO and DA-CoO for selective oxidation of ethylbenzene, a few contrast experiments were conducted. First, a reaction was designed which with commercial CoO and additional DA as catalyst to exclude the impact of dissociative DA. From the results with conversion of 17%, it can deduce that the

Table 1   Selective oxidation of ethylbenzene with different catalysts.
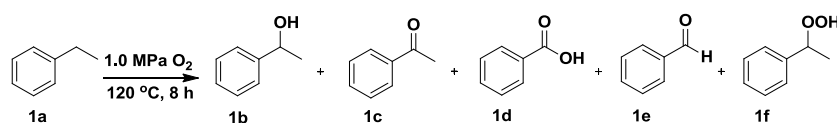
Entry	Catalyst	Conv. (%)	Distribution of products (%)				
			1b	1c	1d	1e	1f
1	BA-CoO	50	16	79	4	1	0
2	DA-CoO	53	13	78	7	1	1
3	CoO	18	27	69	-	1	3
4[a]	CoO	17	27	64	-	2	7
5[b]	CoO	20	27	66	1	1	5
6[c]	CoO	45	14	81	1	2	2

Reaction conditions: catalyst (20 mg), ethylbenzene (80 mmol), 1.0 MPa O_2, TBHP (80 mg) as initiator; [a]1.6 mg DA was added; [b]the CoO was impregnated with DA at room temperature; [c]the CoO was impregnated with DA at 250 °C.
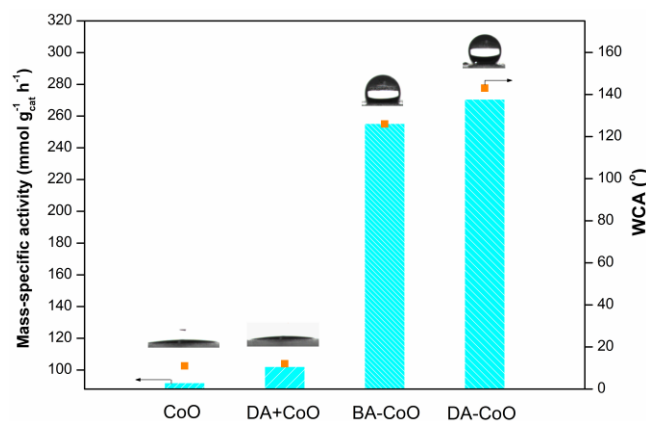
Fig. 5. Mass-specific activity (mmol g_{cat}^{-1} h^{-1}) of the CoO and amines modified CoO for ethylbenzene oxidation with the variable WCA.

dissociative DA had no vital effect on the reaction (entry 4). Then, the hydrophilic and hydrophobic properties of CoO for the reaction were researched. When the commercial CoO was impregnated with 2-octanol and DA with being stirred at room temperature for 5 h, it still showed a hydrophilic surface with a WCA of 12° (Fig. S11), and the catalytic conversion was 20% (entry 5). However, when the commercial CoO was impregnated with 2-octanol and DA at 250^oC for 5 h, the WCA reached 143°, which means the hydrophobic property of the amine treated commercial CoO (Fig. S12). With this hydrophobic catalyst, the conversion of ethylbenzene increased from 18% to 45%, the selectivity of acetophenone increased from 69% to 81% (entry 6). Besides, as showed in Fig. 5, the mass-specific activity for CoO was 92 mmol g_{cat}^{-1} h^{-1}, after modified with DA, which increased to 271 mmol $g_{cat}^{-1} h^{-1}$ for DA-CoO, along with the increase of WCA from 11° to 143°. To sum up, these contrast results can verify that the acquisition of the hydrophobic surface is of vital importance for the improvement of the catalytic activity. Furthermore, the reusability of the DA-CoO was investigated by recycling experiments. The after reaction catalyst was regenerated through impregnated with 2-octanol and DA at 250^oC. After the regeneration process, the catalyst could be reused for at least 4 times.
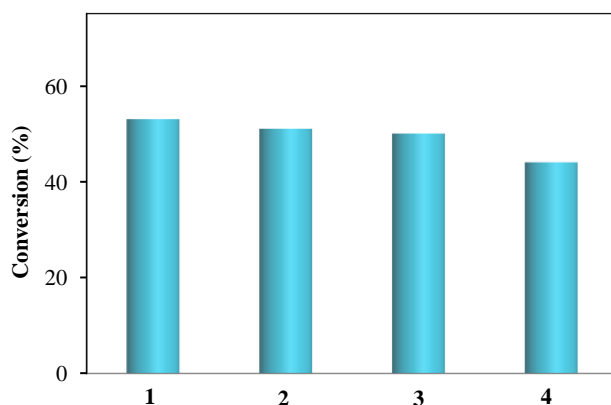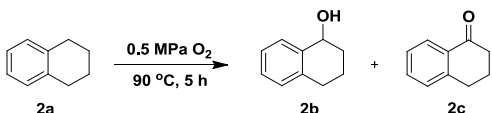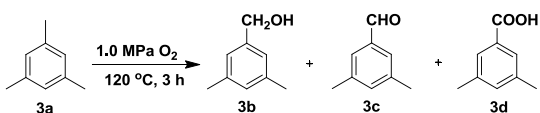

Fig. 6. Cycle tests on DA-CoO. Reaction conditions: ethylbenzene (80 mmol), catalyst (20 mg), 1.0 MPa O_2, TBHP (80 mg) as initiator, 120^oC, 8 h.

Table 2 Comparative selective oxidation of tetralin and mesitylene with different catalysts.

| Entry | Catalyst | Conv. (%) | Distribution of products (%) | | | Mass-specific activity |
			2b	2c	Others	(mmol $g_{cat}^{-1} h^{-1}$)
1	CoO	32	37	57	6	256
2	DA-CoO	63	32	56	12	503

| Entry | Cat. | Conv. (%) | Distribution of products (%) | | | | Mass-specific activity |
			3b	3c	3d	Others	(mmol $g_{cat}^{-1} h^{-1}$)
1	CoO	25	34	35	29	2	306
2	DA-CoO	52	15	17	55	13	637

Reaction conditions: catalyst (20 mg), reactant (74 mmol), TBHP as initiator (80 mg), O_2 as oxidant.

In the distribution test, it could be observed that the hydrophobic DA-CoO could remain in a highly distribution state in the organic phase (Fig. S14). While for the commercial hydrophilic CoO nanoparticle, it distributed in the water phase. This experiment was in accordance with the WCA test, confirming the high affinity towards the organic molecule and the strong water repellent ability. This characteristic could hinder the adsorption of the inevitable water on the active site and could be dispersed more uniform during the reaction as our previous report. Accordingly, excellent catalytic performance was achieved with the hydrophobic catalyst.

Not only be an active catalyst for ethylbenzene oxidation, the hydrophobic DA-CoO was also an active catalyst for the selective oxidation of tetralin and mesitylene (Table 2). It showed similar effect between the hydrophobic and hydrophilic catalysts under the same conditions, the conversion of tetralin and mesitylene increased from 32% to 63% and 25% to 52%, respectively. In addition, the selectivity of deep oxidation products also increased, in accordance with the ethylbenzene oxidation.

In summary, through surface modification, a new hydrophobic CoO nanoparticle coating by amines was synthesized, which showed high activity for selective oxidation of aromatic hydrocarbon. The amines coating on the surface of the CoO nanoparticles brought the hydrophobic property, which owned a WCA of 143°. It was believed that the hydrophobic property of the CoO surface is an important factor of the high catalytic performance.

References

[1] M. M. Sharma, T. Sridhar, *Ind. Eng. Chem. Res*., **2000**, 39(11), 3958-3997.

[2] J. M. Thomas, R. Raja, G. Sankar, R. G. Bell, *Nature*, **1999**, 398, 227-230.

[3] T. Punniyamurthy, S. Velusamy, J. Iqbal, *Chem. Rev*., **2005**, 105, 2329-2363.

[4] M. S. Hamdy, A. Ramanathan, T. Maschmeyer, U. Hanefeld, J. C. Jansen, *Chem. -Eur. J*., **2006**, 12, 1782-1789.

[5] C. Chen, J. Xu, Q. Zhang, Y. Ma, L. Zhou, M. Wang, *Chem. Commun*., **2011**, 47, 1336-1338.

[6] X. Li, L. Zhou, J. Gao, H. Miao, H. Zhang, J. Xu, *Powder Technol*., **2009**, 190, 324-326.

[7] G. Zhang, D. Wang, P. Feng, S. Shi, C. Wang, A. Zheng, G. Lü, Z. Tian, *Chin. J. Catal*., **2017**, 38, 1207-1215.

[8] M. Y. Zhang, L. F. Wang, H. B. Ji, B. Wu, X. P. Zeng, *J. Nat. Gas Chem*., **2007**, 16, 393-398.

[9] C. Zhang, Y. Bai, Y. Yin, J. Gu, Y. Sun, *Korean J. Chem. Eng*., **2011**, 28, 602-607.

[10] D. N. Srivastava, N. Perkas, G. A. Seisenbaeva, Y. Koltypin, V. G. Kessler, A. Gedanken, *Ultrason. Sonochem*., **2003**, 10, 1-9.

[11] L. Zhou, J. Xu, H. Miao, F. Wang, X. Li, *Appl. Catal. A*, **2005**, 292, 223-228.

[12] T. Liu, H. Cheng, L. Sun, F. Liang, C. Zhang, Z. Ying, W. Lin, F. Zhao, *Appl. Catal. A*, **2016**, 512, 9-14.

[13] H. Li, L. Li, Y. Li, *Nanotechnol. Rev*., **2013**, 2, 515-518.

[14] W. Shi, L. Cao, H. Zhang, X. Zhou, B. An, Z. Lin, R. Dai, J. Li, C. Wang, W. Lin, *Angew. Chem. Int. Ed*., **2017**, 56, 9704-9709.

[15] C. Chen, J. Xu, Q. Zhang, H. Ma, H. Miao, L. Zhou, *J. Phys. Chem. C*, **2009**, 113, 2855–2860.

[16] M. Wang, C. Chen, Q. Zhang, Z. Du, Z. Zhang, J. Gao, J. Xu, *J. Chem. Technol. Biotechnol*., **2010**, 85, 283-287.

[17] C. Chen, S. Shi, M. Wang, H. Ma, L. Zhou, J. Xu, *J. Mater. Chem. A*, **2014**, 2, 8126-8134.

[18] L. Wang, F.-S. Xiao, *ChemCatChem*, 2014, 6, 3048-3052.

[19] T. Li, J. Wang, F. Wang, L. Zhang, Y. Jiang, H. Arandiyan, H. Li, *ChemCatChem*, **2019**, 11, DOI: 10.1002/cctc.201801925.

[20] J. Zhang, X. Liu, R. Blume, A. Zhang, R. Schlögl, D. S. Su, *Science*, **2008**, 322, 73-77。

[21] F. Studt, F. Abild-Pedersen, T. Bligaard, R. Z. Sorensen, C. H. Christensen, J. K. Norskov, *Angew. Chem. Int. Ed*., **2008**, 47, 9299-9302.

[22] L. D. Ellis, R. M. Trottier, C. B. Musgrave, D. K. Schwartz, J. W. Medlin, *ACS Catal*., **2017**, 7, 8351-8357.

[23] X. Jia, J. Ma, F. Xia, Y. Xu, J. Gao, J. Xu, *Nat. Commun*., **2018**, 9, 933.

[24] M. Tamura, R. Kishi, Y. Nakagawa, K. Tomishige, *Nat. Commun.*, **2015**, 6, 8580.

[25] L. Li, X. Sun, X. Qiu, J. Xu, G. Li, *Inorg. Chem.*, **2008**, 47, 8839-8846.

[26] X. Liu, M. Atwater, J. Wang, Q. Dai, J. Zou, J. P. Brennan, Q. Huo, *J. Nanosci. Nanotechnol.*, **2007**, 7, 3126-3133.

[27] Y. Tian, B. Yu, X. Li, K. Li, *J. Mater. Chem.*, **2011**, 21, 2476-2481.

[28] Z. Xu, C. Shen, Y. Hou, H. Gao, S. Sun, *Chem. Mater.*, **2009**, 21, 1778-1780.

[29] B. Ernst, S. Libs, P. Chaumette, A. Kiennemann, *Appl. Catal. A.*, **1999**, 186, 145-168;

[30] T. Garcia, S. Agouram, J. F. Sánchez-Royo, R. Murillo, A. M. Mastral, A. Aranda, I. Vázquez, A. Dejoz, B. Solsona, *Appl. Catal. A.*, **2010**, 386, 16-27;

[31] Y. Chen, S. Zhao, Z. Liu, *Phys. Chem. Chem. Phys.*, **2015**, 17, 14012-14020.

[32] K. B. Klepper, O. Nilsen, H. Fjellvåg, *Thin Solid Films*, **2007**, 515, 7772-7781.

脂肪胺修饰的CoO纳米粒子催化分子氧选择氧化芳香烃

刘 梦[a,b], 石 松[a,#], 赵 丽[a,b], 陈 晨[a,c], 高 进[a], 徐 杰[a,*]

[a]中国科学院大连化学物理研究所催化基础国家重点实验室, 洁净能源国家实验室(筹), 辽宁大连 116023

[b]中国科学院大学, 北京 100049

[c]宁波大学,材料科学与化学工程学院，浙江宁波 315211

摘要:通过分子氧实现烃类的选择氧化在学术研究和工业应用中均为十分重要的课题。金属氧化物在催化烃类选择氧化过程中具有较高的催化活性，包括锰氧化物（MnO_x）、钴氧化物（CoO_x）以及铜氧化物（CuO_x）等。其中CoO_x纳米粒子的活性较高，关于其粒径、孔结构以及组分等影响因素均有文献进行研究。在多相催化反应中，催化剂的微环境对催化反应性能有直接的影响。烃类氧化的反应过程中生成的产物分子，尤其是水分子，极性大于底物分子，使得具有疏水微环境催化剂对该反应有利。而CoO_x由于表面羟基的存在呈亲水性质。因此，如何对CoO_x进行修饰而制备疏水的CoO_x纳米粒子从而提高其烃类氧化的活性，成为十分重要的课题。

本文利用有机胺对CoO_x纳米粒子进行有机修饰，得到了丁胺修饰的BA-CoO和十二胺修饰的DA-CoO，静态水滴接触角分别为126°和143°，证明了其表面呈疏水性质。通过X射线粉末衍射测定了催化剂为立方相CoO，透射电镜表征了纳米粒子的形貌和粒径，并且红外光谱和X射线光电子能谱证明了纳米粒子中有机胺的存在。

在催化芳香烃类分子氧氧化反应中，疏水性的DA-CoO和BA-CoO均表现出比亲水性的CoO更高的催化活性，其中DA-CoO催化乙苯转化率为53%，苯乙酮选择性为78%；而亲水的CoO对应的转化

率和选择性分别为18%和69%。通过有机胺修饰的CoO纳米粒子提高了在烃类催化氧化中的活性，这种有机胺修饰的方法为其它金属氧化物的疏水性修饰提供了参考。

关键词:烃氧化；疏水修饰；有机胺修饰；钴氧化物；表面修饰

Aliphatic amines modified CoO nanoparticles for catalytic oxidation of aromatic hydrocarbon with molecular oxygen

Meng Liu, Song Shi[#], Li Zhao, Chen Chen, Jin Gao, Jie Xu*

Dalian Institute of Chemical Physics, Chinese Academy of Sciences

University of Chinese Academy of Sciences
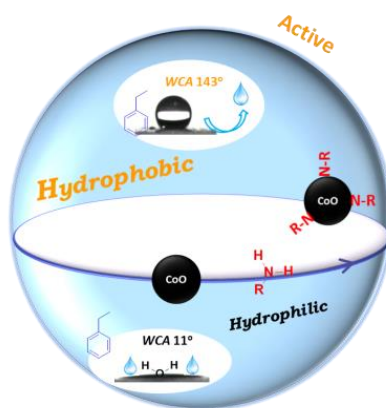
The amines modified CoO nanoparticles showed the hydrophobic properties owning water contact angle of 143°, which accompanied with better performance than the hydrophilic commercial CoO nanoparticles in the hydrocarbon oxidation process.